

# STRUCTURE, THERMAL, AND MECHANICAL PROPERTIES OF INTERFACES IN PMC: A MOLECULAR SIMULATION STUDY

K. Sebeck, C. Shao, J. Kieffer\*

Department of Materials Science and Engineering, University of Michigan, Ann Arbor, MI 48109, USA

\* Corresponding author ([kieffer@umich.edu](mailto:kieffer@umich.edu))

## 1 Introduction

The properties of polymer-matrix nano-composites are predominantly controlled by phenomena in the interfacial regions between polymer and reinforcing particles, which constitute a large volume fraction of these materials. To improve the design of nano-composites a thorough understanding of how the structure and chemical constitution of these interfacial regions affects the thermal, mechanical, and electrical properties these composites is needed. By the very nature of these interfaces, this knowledge must be obtained at the molecular level. Moreover, interfaces are buried, and accessing them for experimental inspection invariably requires disturbance, if not destruction of the molecular structure surrounding the interfaces. Hence, it is of great importance to complement experimental techniques of investigation with computer simulations.

One of the principal impediments for studying interfaces using molecular simulations is the difficulty in developing realistic models to describe the interactions between atoms across an interface between dissimilar materials. In recent years, however, there has been significant progress in developing suitable interatomic potentials [1]. Thus far, the emphasis has been on the study of interfaces between two different inorganic compounds, or on hydrocarbon/carbon interfaces [1-4]. Polymer/metal interfaces are furthermore complicated to simulate due to the large disparity in the physical properties, and corresponding differences in the forms of the interatomic potential used to describe the respective bulk interactions.

## 2 Research Approach and Methodologies

To carry out such simulations at the necessary level of detail and accuracy, we developed a multi-scale

simulation framework for the investigation of interfacial regions in nano-composites. Our objective is to understand the nature and properties of these interfaces and create a toolset for the predictive design of novel composite materials. Our framework includes (i) first-principles density functional theory calculations to develop a detailed description of the interactions and chemical bonding across interfaces, in particular between dissimilar materials; (ii) large-scale molecular dynamics simulations, based on the reactive interatomic potential we have developed in our group, to gain realistic atomistic representations of the polymer/nano-particle interfaces and to compute the mechanical, thermal, dielectric, and transport properties of the composites; and (iii) a coarse-graining particle dynamics scheme to account for slower structural relaxation processes that contribute to the development of interfacial regions. The coarse-graining scheme is designed to accelerate the evolution of the simulated configurations. To this effect, molecules or groups of atoms are represented as single particles that interact via potentials [5].

Using these methodologies, our research approach consists of first generating realistic interfacial structures by reproducing the transport and reaction processes that govern structural developments in the actual systems, and then use these structural models to study interfacial phenomena and predict the properties of nano-composite materials [5].

In this paper we report our findings concerning metal-polymer interfaces. We investigated the structure and properties of alkane chains with variable chain length that are deposited on the (100) surface of copper. Structures are simulated using an embedded atom method (EAM) potential for copper-copper interactions [6], the COMPASS potential to describe hydrocarbon interactions [7], and a suitably parametrized 12-6 Lennard-Jones potential is

utilized for hydrocarbon-metal nonbonded interactions. No reactions or hydrogen bonding occur between metal and alkane, making the Lennard-Jones potential a reasonable approximation for the governing van der Waals forces. Periodic boundary conditions are assumed in all directions.

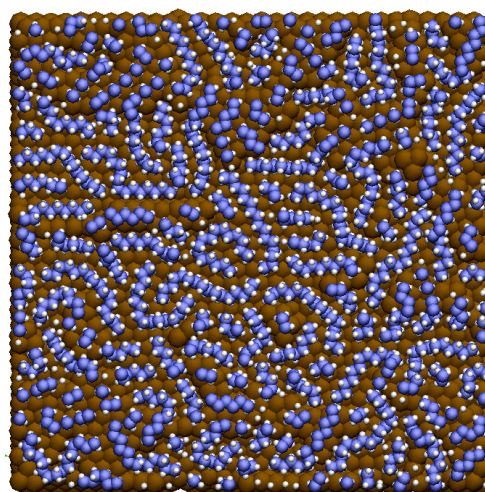
### 3 Results and Discussion

#### 3.1 Surface Wetting Behavior

The extent of contact between polymer chains and the surface depends on the structural compatibility between the two phases and the degree of flexibility and/or mobility of the polymer on the surface. When simulating the deposition of simple alkane chains  $C_nH_{n+2}$ , with  $n$  varying between 8 and 16, we found that the longer chains tend to align by adapting to the periodicity of the metal surface, and form a pattern of small regular domains. In this case, much better contact is established between polymer and metal surface. Polymer chains tend to adhere to the substrate surface over their entire length. The overall energy of this surface layer is lowered by achieving both epitaxy with the metal lattice and order among polymer chains themselves over the spatial extent of each domain. This is shown in Fig. 1, where only the top layer of metal atoms and the layer of polymer chains immediately in contact with the metal is displayed. (The bulk of the polymer is not shown so as to not obstruct viewing.)

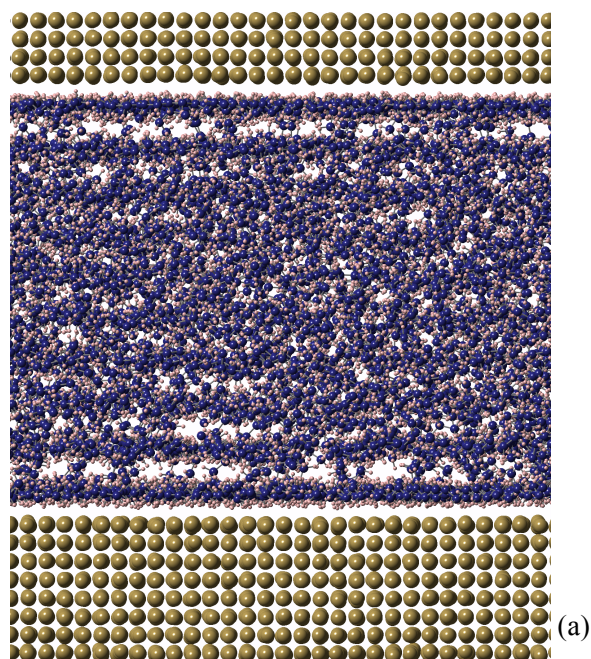
#### 3.2 Mechanical Properties of Interfaces

Another striking behavior we discovered is that the polymer units in immediate contact with the substrate surface assume a structure that is to varying degrees incompatible with the bulk polymer. A gap develops between the polymer immediately adhering to the metal surface and the bulk of the polymer. While this is understandable for the case of longer alkanes, where two-dimensional nano-crystalline domains develop at the interface, this behavior even persists for polymer that bonds to the surface of the substrate via reactive end groups [5]. Hence, the weakest mechanical link in a polymer matrix composite in which polymer chains can order congruently with the surface structure of the embedded particles, is most likely between the adsorbed layer and the bulk polymer.



**Fig. 1** Top view of the Cu (100) surface (brown atoms) wetted by  $C_{16}H_{34}$ . Only polymer chains in direct contact with the metal surface are shown.

Moreover, a high degree of structural compatibility between metal surface and polymer induces a distinctive layering in the polymer in the vicinity of the interface, which affects both the thermal and mechanical properties of the material. This is shown in Fig. 2, for the case of  $C_{16}H_{34}$  and  $C_8H_{18}$  polymer. Interestingly, polymer chains that span across several layers, i.e., that provide mechanical strengths by creating entanglement between layers, do so by assuming a “staircase” pattern (Fig. 3).



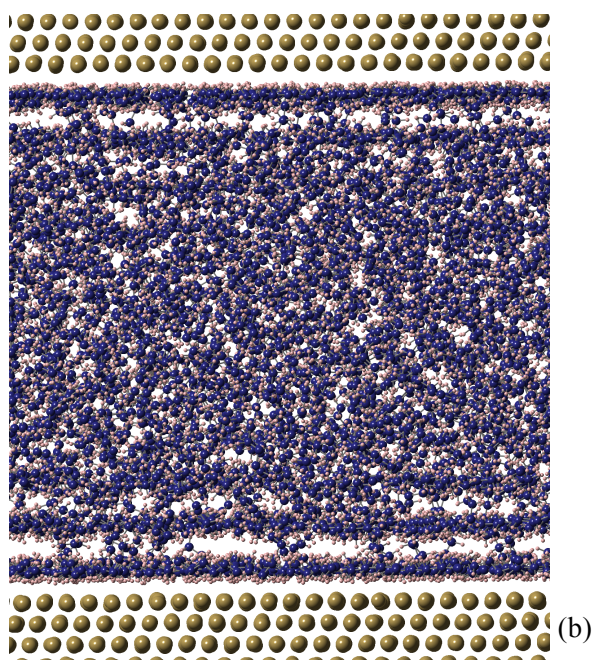


**Fig. 2** Cross-sectional side view of  $C_{16}H_{34}$ , sandwiched between Cu (100) surfaces (a) and between Cu (111) surfaces (b), showing the distinctive layering of polymer near the interface. The layering subsides with increasing distance from the interface.

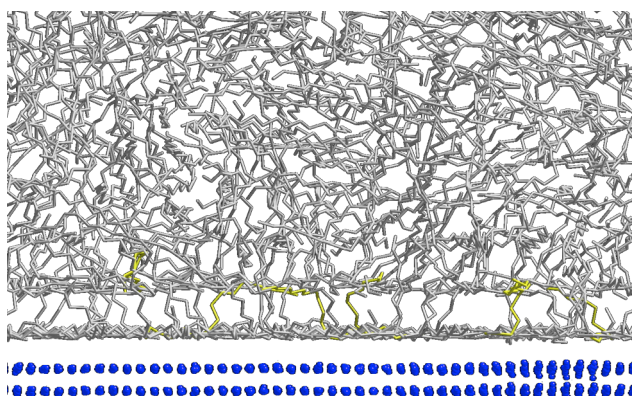


**Fig. 3** Side view of the Cu (111) surface (blue atoms) as wetted by  $C_{16}H_{34}$  polymer, with “staircase” chains highlighted in yellow

The pronounced layering of polymer chains near interfaces is also evident from quantitative measures. For example, the planar pair correlation functions,  $g(r)$ , evaluated for thin (approximately intermolecular spacing) two-dimensional slices that are parallel to the interfaces, as a function of distance from the interface, are shown in Fig 4. The

distribution function in the layers closest to the copper surfaces shows more sharply defined peaks, indicating a more ordered structure. This behavior is most obvious for  $C_8H_{18}$ , indicating shorter chain lengths are more strongly affected by the presence of an ordered surface.

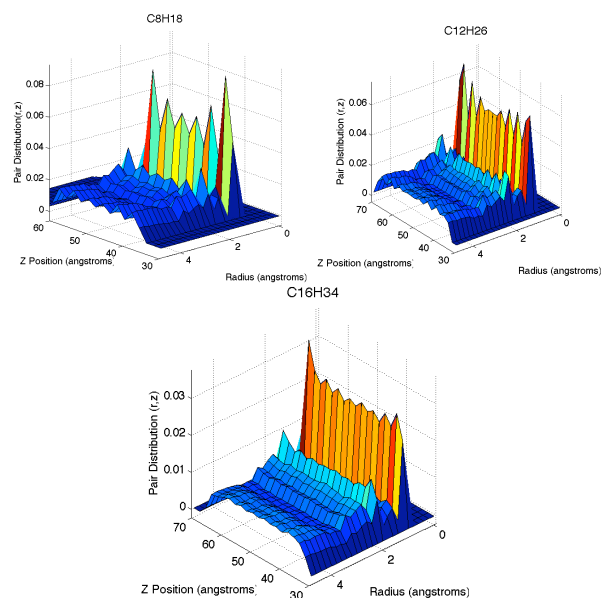


**Fig. 4** Pair correlation functions,  $g(r)$ , as a function of  $z$ -position for  $C_8H_{18}$  (top left),  $C_{12}H_{26}$  (top right) and  $C_{16}H_{34}$  (bottom). Near copper surfaces  $g(r)$  have sharper peaks, most evident for short chains.

Rather than using end-to-end or end to arbitrary point vector analysis to describe chain orientation, a plane of best fit was determined for each linear alkane molecule. This is done using a principal component analysis (PCA), wherein an eigenvalue decomposition of the entire set of three-dimensional atomic coordinates associated with a given alkane chain identifies the vectors describing the plane associated with the largest two-dimensional expanse of this chain [8]. “Flatness” is calculated by the sum of the squares of displacements of atomic positions perpendicular to this plane,  $\langle d^2 \rangle$ . Smaller values of  $\langle d^2 \rangle$  indicate a higher degree of planarity. This plane can also be used to determine the dihedral angle between the alkane chain and the metal surface. The average dihedral angle and degree of flatness as a function of  $z$  position are plotted in Figs. 5 6, respectively.

Chains adhering to the metal surfaces have an average dihedral angle of nearly zero between the metal surface and the best-fit plane. As the distance from the interface increases, the average angle approaches  $45^\circ$ , indicating random chain orientation. This is true for all chain lengths. The influence of the proximity to the metal interface on chain flatness is less apparent (Fig. 6). However, the PCA plane more closely fits alkane chains in the first layer adhering to the metallic surface. Furthermore, chains crossing the gap region show the poorest fit, which is again most obvious the shorter the chain length. Finally, note that for polymer chains to simultaneously have their center of mass closely positioned to the interface and be characterized by a large dihedral angle, the chains must exhibit sharp kinks. This latter observation allowed us to identify the staircase configurations that constitute a significant portion of the mechanical links between layers near the interfaces.

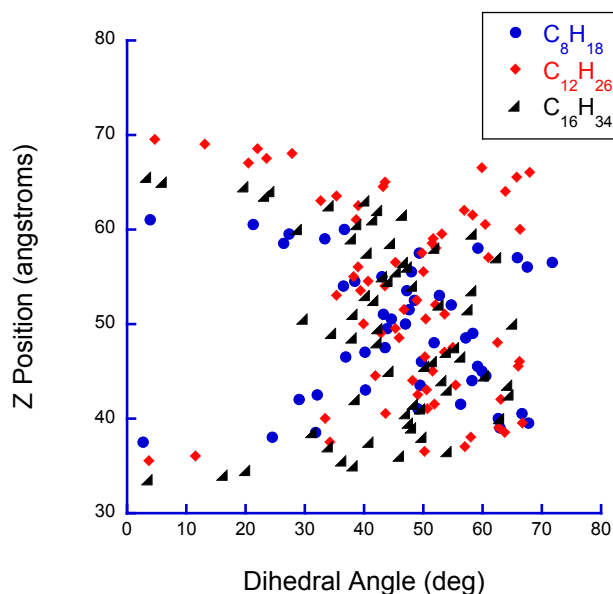


**Fig. 5** Distribution of the average dihedral angle of best-fit planes as a function of the center of mass z-position of  $C_8H_{18}$  (blue circle),  $C_{12}H_{26}$  (red diamond) and  $C_{16}H_{34}$  (black triangle). Near the interfaces ( $z \sim 30 \text{ \AA}$  and  $z \sim 70 \text{ \AA}$ ) the dihedral angle is near zero, while chains in the bulk are randomly oriented with an average dihedral angle of  $45^\circ$ .

### 3.3 Thermal Properties of Interfaces

We determined the thermal conductivity of the polymer near interfaces as well as the thermal boundary resistance at the metal-polymer interface using the Müller-Plathe method, which is based on non-equilibrium molecular dynamics simulations. Our findings reveal strong correlations with mechanical properties. Generally, the thermal conductivity increases sub-linearly with the polymer chain length. This indicates an asymptotic approach towards a plateau value for a particular chain length, beyond which the thermal conductivity becomes independent of the chain length. Preliminary simulation results for systems with longer alkane chains corroborate this hypothesis. However, further equilibration of the simulated configurations is necessary to ascertain the accuracy of these findings. This is particularly important for configurations containing long polymer chains, as the entanglement of these molecules prevents a swift approach of their equilibrium structures.

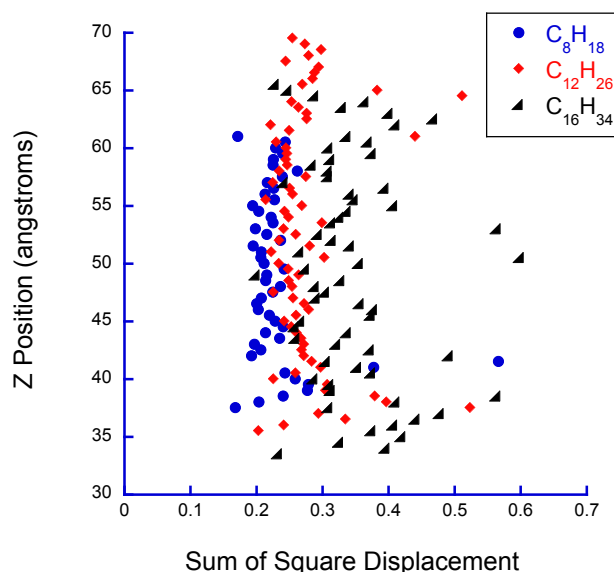


**Fig. 6** Distribution of “flatness”  $\langle d^2 \rangle$  as a function of the center of mass z-position of  $C_8H_{18}$  (blue circle),  $C_{12}H_{26}$  (red diamond) and  $C_{16}H_{34}$  (black triangle). Chains near copper surfaces ( $z \sim 30 \text{ \AA}$  and  $z \sim 70 \text{ \AA}$ ) have low values of  $\langle d^2 \rangle$ , indicating a greater degree of flatness. This effect is more pronounced for shorter chains.

The thermal boundary resistance is governed by the type of metal surface, which controls the organization of the polymer in the wetting layer and the strength of the chemical bonding across the interface [9]. Interestingly, the thermal conductivity across the polymer layer sandwiched between metal surfaces is consistently higher for the (111) surface compared to the (100), which is probably due to the translation of the structural congruency achieved with the (111) surface farther into the bulk of the polymer.

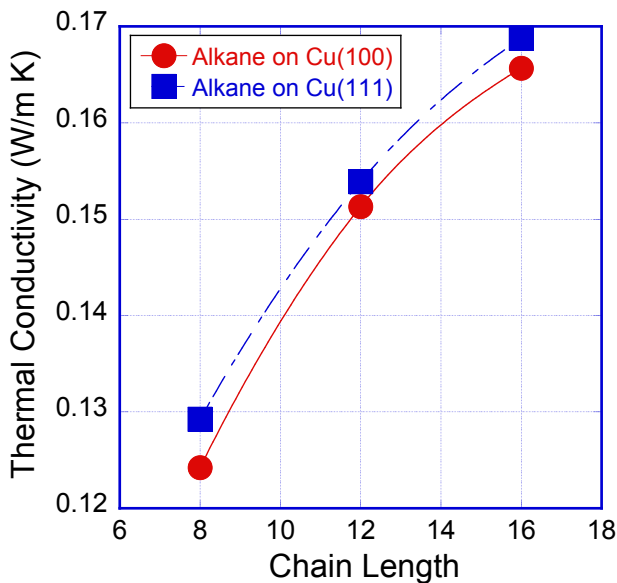


**Fig. 7** Thermal conductivity of alkane chains in the gap between two metal surfaces, as a function of the alkane chain length.

#### 4. Summary

Using atomistic simulations we generate realistic models of the interfacial structures by reproducing the underlying reaction and transport processes. These models serve to understand and predict interfacial behaviors. We observe pronounced polymer chain layering and the formation of an incompatibility gap near the interface that govern their thermo-mechanical properties.

#### References

[1] S.Q. Wang and H.Q. Ye, "Theoretical studies of solid-solid interfaces," *Curr. Op. in Sol. State & Mat. Sci.* **10**, 26 (2006)

[2] S. Namilae and N. Chandra, "Multiscale Model to Study the Effect of Interfaces in Carbon anotube-Based Composites," *Transaction of the ASME*, **127**, 222 (2005)

[3] V.A. Harmandaris, K.C. Daoulas and V.G. Mavrantzas, "Molecular dynamics simulation of a polymer melt/solid interface: local dynamics and chain mobility in a thin film of polyethylene melt adsorbed on graphite," *Macromol.* **38**, 5796 (2005)

[4] K.C. Daoulas, V.A. Harmandaris and V. G. Mavrantzas, "Detailed atomistic simulation of a polymer melt/solid interface: structure, density and conformation of a thin film of polyethylene adsorbed on graphite," *Macromol.* **38**, 5780 (2005)

[5] S. Maiti, C. Shankar, P. Geubelle, and J. Kieffer, "Continuum and molecular-level modeling of fatigue crack retardation in self-healing polymers," *J. Eng. Mat. Tech.* **128**, 595 (2006)

[6] J.B. Adams, S.M. Foiled and W.G. Wolfer, "Self-diffusion and impurity diffusion of FCC metals using the 5-frequency model and the Embedded Atom Method," *J. Mater. Res.* **4**, 102 (1989)

[7] H. Sun, "COMPASS: An ab Initio Force-Field Optimized for Condensed-Phase Applications – Overview with Details on Alkane and Benzene Compounds," *J. Phys. Chem. B* **102**, 7338 (1998)

[8] H. Abdi, L.J. Williams, "Principal Component Analysis," *Wiley Interdisciplinary Reviews: Computational Statistics*, **2**, 433 (2010)

[9] C. Shao, K. Becker, J. Kieffer, "Structure and Properties of Alkane-Metal interfaces by Molecular Dynamics Simulations," *in preparation*.